ISSN 1573-160X, *PHYSICAL OCEANOGRAPHY*, Vol. 33, Iss. 1, pp. 185-200 (2026)
Original Russian Text © D. V. Kalinskaya, A. S. Papkova, 2026,
published in *Morskoy Gidrofizicheskiy Zhurnal*, 2025, Vol. 42, Iss. 1, pp. 144–161

Original article

Assessment of the Error in Satellite Measurements of Atmosphere Optical Characteristics and Remote Sensing Reflectance of the Sea of Japan for Spring Period, 2023

D. V. Kalinskaya ✉, A. S. Papkova

Marine Hydrophysical Institute of RAS, *Sevastopol*, *Russian Federation*
✉ *kalinskaya_d_v@mail.ru*

Abstract
Purpose. The purpose of the study is to assess the errors in satellite measurements of atmospheric optical characteristics and remote sensing reflectance of the Sea of Japan in the presence of dust aerosol in the atmosphere.
Methods and Results. To perform a comparative analysis and to assess the error in satellite measurements of atmospheric optical characteristics and remote sensing reflectance, the following information was used: photometric measurement data from the AERONET international aerosol monitoring network, the MODIS/Aqua spectroradiometer, and the VIIRS radiometer on the Suomi NPP satellite; data from NOAA-20 and NOAA-21 on the concentration of suspended particles PM2.5 and PM10 derived from modeling of atmospheric dynamics (data of the HYSPLIT and SILAM models). A comparative analysis of satellite and *in situ* data made it possible to identify the dates of anomalous dust impact on the remotely determined optical characteristics of water. Besides, different estimates of the area covered completely and partially by dust were obtained on one and the same day. This confirms different aerosol loading in the atmosphere over the Sea of Japan, as well as the spatial variability of the main aerosol optical characteristics during dust transport from the Asian deserts.
Conclusions. A comparative analysis of satellite and *in situ* photometric data has supported the fact that in the presence of dust transport, the error of standard atmospheric correction increases sharply in the UV part of the spectrum. Calculation and approximation of the obtained values using a power-law function show that for the entire region of the Sea of Japan, the value of atmospheric correction error is of the form λ^{-7}. As for the studied dust episode, the analytically assessed error in the VIIRS/NOAA satellite measurements of the sea remote sensing reflectance constitutes approximately 70% in the shortwave part of the spectrum, up to 47% in the visible part of the spectrum, and 24% in the long-wave part of the spectrum, relative to the *in situ*-measured values of this characteristic.

Keywords: AERONET, Sea of Japan, dust aerosol, optical characteristics, remote sensing reflectance, atmospheric correction of remote sensing reflectance

Acknowledgements: The study was carried out within the framework of the theme of the state assignment of FSBSI FRC MHI FNNN-2024-0012 “Analysis, nowcast and forecast of the state of hydrophysical and hydrochemical fields of marine water areas based on mathematical modeling using the data of remote and contact measurement methods”. The author is grateful to S.M. Sakerin and D.M. Kabanov for providing the SPM photometer and its software, as well as to Tom Kucsera, Brent Holben, Giuseppe Zibordi and the group of Gene Feldman (NASA) for providing the AOD data, and calculating the BTA data.

For citation: Kalinskaya, D.V. and Papkova, A.S., 2026. Assessment of the Error in Satellite Measurements of Atmosphere Optical Characteristics and Remote Sensing Reflectance of the Sea of Japan for Spring Period, 2023. *Physical Oceanography*, 33(1), pp. 185-200.

Introduction

According to data available online and in the press, severe dust storms from the Gobi Desert affected East Asia at least four times during the spring of 2023,

starting on 10 March 2023. One such dust outflow event, accompanied by strong winds, was recorded from April 8 to 13, 2023. During this period, due to the influence of an active cyclone in Mongolia, which arose from a high-altitude frontal zone formed to the south, an intensive outflow of dust and sand occurred, affecting most of the Yangtze River basin in China, the Korean Peninsula, Japan, and other areas. The dust cloud moved towards China and South Korea on April 11, which was confirmed by anomalously high air quality index values corresponding to an extremely hazardous level of suspended particles (PM10 and PM2.5). Subsequently, the dust storm was noted in Fukuoka, Japan, on the morning of April 12. According to data from the World Meteorological Organization Regional Specialized Meteorological Center for Sand and Dust Storms and the Air Self-Defense Force (ASDF), the maximum concentration of PM10 particles exceeded 2000 μg/m³ in many parts of Northern China, reaching 1500 μg/m³ in Beijing (https://meteoinfo.ru/novosti/99-pogoda-v-mire/19174-pylnaya-burya-v-azii).
A massive dust cloud was recorded in satellite observations in the atmosphere towards Hokkaido Island, as well as over Sakhalin Island. Yellow-brown dust was also recorded over the Kuril Islands.

It is worth noting that a number of studies have previously been conducted considering the influence of dust aerosols on the ecosystem of this region [1–4]; however, an analytical assessment of this influence on the error of atmospheric correction has not been provided. The frequent occurrence of large amounts of absorbing dust aerosol over the sea surface significantly complicates satellite measurements of spectral sea color in the study region, making the stated task relevant [5, 6]. Russian scientists from the V.I. Ilyichev Pacific Oceanological Institute, Far Eastern Branch of RAS, are actively engaged in studying the Sea of Japan using satellite and *in situ* (shipboard) measurements of its optical characteristics. In studies [7–10], which present a number of quasi-analytical bio-optical regional algorithms, a long-term analysis of shipboard measurements indicates that at the beginning of the spring period, maximum chlorophyll a concentrations are observed in the surface layer. Work [9] mentions the occurrence of significant errors in the presence of absorbing aerosol in the atmosphere. An overestimation of satellite estimates of chlorophyll a concentration after aerosol enters the surface layer of the Sea of Japan in spring is described in [10].

In situ measurements for atmospheric parameters used data from stations of the international aerosol monitoring network AERONET (Level 1.5 and Level 2) [11]. In April 2023, AERONET stations near the coast of the Sea of Japan were operational, as shown in Fig. 1. For a comprehensive assessment of the dust aerosol impact on the Sea of Japan waters, satellite data with the highest quality (Level 2) were selected, as only these allow for high-quality cloud screening (pixel screening) and correction for cloud contamination. For the comparison of satellite and *in situ* measurements, data from MODIS/Aqua [12], VIIRS [13, 14], and AERONET were chosen. Consequently, to assess dust transport over the Sea of Japan during the study period, this paper provides an analysis of optical characteristics for the following AERONET stations: Gangneung_WNU (37.8°N, 128.9°E) [Gangneung, Korea], KORUS_UNIST_Ulsan (35.6°N, 129.2°E) [Ulsan, Korea], Noto (37.3°N, 137.1°E) [Noto, Japan], Niigata (37.8°N, 138.9°E) [Niigata, Japan], Hokkaido_University (43.1°N, 141.3°E) [Sapporo, Japan]. For clarity, AERONET stations with Level 2 processing are highlighted in red in Fig. 1.

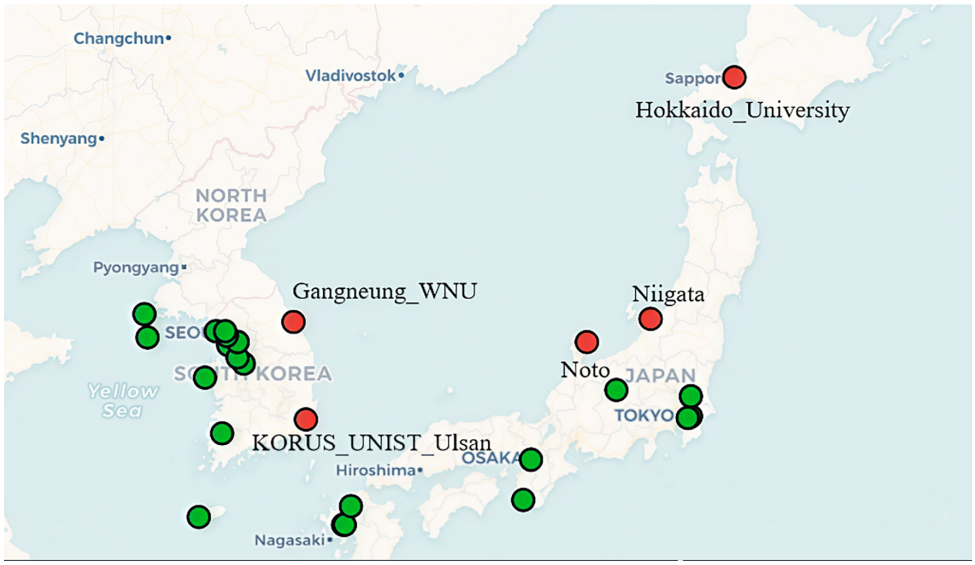

F i g. 1. AERONET stations map for the Sea of Japan region, April 2023 (https://aeronet.gsfc.nasa.gov/)

This work aims at assessing the error in satellite measurements of atmospheric optical characteristics and remote sensing reflectance of the Sea of Japan waters in the presence of dust aerosol in the atmosphere.

Research methods and instruments

The following types of data were applied in the work: photometric measurements from stations of the international AERONET network, the MODIS/Aqua spectroradiometer, the VIIRS/Suomi NPP radiometer, and NOAA-20 and NOAA-21 [15, 16]; and data from the kinematic models Hybrid Single-Particle Lagrangian Integrated Trajectory (HYSPLIT) and System for Integrated Modeling of Atmospheric Composition (SILAM). Suspended particles are among the atmospheric pollutants most commonly characterized by mass concentrations.

Work [17] shows the calculation of the error (r) in standard atmospheric correction of satellite data arising from non-uniform aerosol distribution (stratification) under weak light absorption. It is important to note that the spectral properties of aerosol absorption are directly related to its microphysics, which, in turn, depends on dust sources and atmospheric processes.

To calculate aerosol optical depth (AOD) in this study, measurements from the CIMEL photometer in the spectral range 340–1020 nm are used. It is important to note that the channel at 936 nm is not used for AOD calculation but serves to determine atmospheric water vapor content [11, 18].

The source of satellite data is the suite of VIIRS radiometers within the Joint Polar Satellite System (JPSS). VIIRS provides Deep Blue NASA Standard Level-2 (L2) aerosol products, including daily satellite measurements of AOD and aerosol characteristics over land and ocean at 6-minute intervals. To obtain AOD values starting from February 17, 2018, the VIIRS Deep Blue Aerosol algorithm is applied [16]. The result of its operation is the L2 Deep Blue dataset, which contains 55 layers and is referenced at the wavelength of 550 nm [14–16]. Application of this algorithm

allows identification of atmospheric aerosol type during daytime in the absence of clouds and snow.

The SILAM software complex, developed by the Finnish Meteorological Institute, is a modern tool for modeling atmospheric pollution. It is successfully used for analyzing the impact of forest fires, volcanic eruptions, dust transport, and other natural and anthropogenic disasters on the state of the atmosphere as a whole. The calculations are based on a combined Lagrangian–Eulerian model, allowing simulation of the dispersion of various pollutants, including aerosols, gases, dust, radionuclides, and allergens. SILAM generates maps of concentrations of fine (PM2.5) and coarse (PM10) particles at a height of 10 m above ground level, effectively visualizing global pollution. The modeled range for PM2.5 and PM10 is 0–2500 μg/m³ [19–22]. Air quality according to the SILAM model is provided by the parameters TVOC and AQI.

The TVOC parameter allows analysis of air for the presence of volatile organic compounds, including benzene and styrene. The measurement range for TVOC is within 0–2.5 mg/m³ [19, 23, 24].

The Air Quality Index (AQI) is an integrated indicator characterizing the overall state of atmospheric air. It is a piecewise linear function of concentrations of sulfur dioxide (SO_2), nitrogen dioxide (NO_2), PM10, PM2.5, carbon monoxide (CO), and ozone (O_3). National air quality standards for each of these pollutants are set by the United States Environmental Protection Agency (EPA). AQI calculation is based on the ratio of the measured average pollutant concentration to its normative (allowable) level [19–21].

To identify sources of various aerosol types over the Sea of Japan, this work uses the HYSPLIT software complex of backward air trajectory modeling [1].

Results

To determine the optical characteristics of dust aerosol over the Sea of Japan in April 2023, the VIIRS/NOAA instrument with 750 m resolution and MODIS/Aqua with 1 km resolution were used. Fig. 2, a presents a satellite image from VIIRS/NOAA, obtained on April 13, where the area for analysis of absorption effects due to the presence of dust aerosol in the atmosphere is highlighted with a red frame. In the figure, an area with a relatively clean atmosphere compared to the dust-covered one is visualized between dust clouds. Due to identical observation conditions, it was decided to compare the "clean" part of the image (with background aerosol dominance in the atmosphere) and the dust-affected area located on the periphery of the framed area. It can be seen that cloudiness does not overlap the highlighted area, allowing an assessment of the influence of dust aerosol on the retrieval of water-leaving remote sensing reflectance ($Rrs(\lambda)$, where λ is the wavelength, nm). Statistical analysis of AOD data, the Ångström exponent (α), and sea remote sensing reflectance was performed using the SeaDAS program (Fig. 2, *b*). Fig. 2, *c*, *d* presents the result of processing satellite data using the MODIS/AIRS algorithm, which shows dust aerosol loading, and the VIIRS Deep Blue algorithm for determining atmospheric aerosol type over the highlighted

[1] Draxler, R.R. and Rolph, G.D., 2013. *HYSPLIT (HYbrid Single-Particle Lagrangian Integrated Trajectory) Model Access via NOAA ARL READY Website*. Silver Spring, MD: NOAA Air Resources Laboratory. [online] Available at: http://ready.arl.noaa.gov/HYSPLIT.php [Accessed: 30 January 2026].

area; markers indicate the location of AERONET stations. According to the presented data, on April 13, the dust plume covered several hundred kilometers of land and sea.

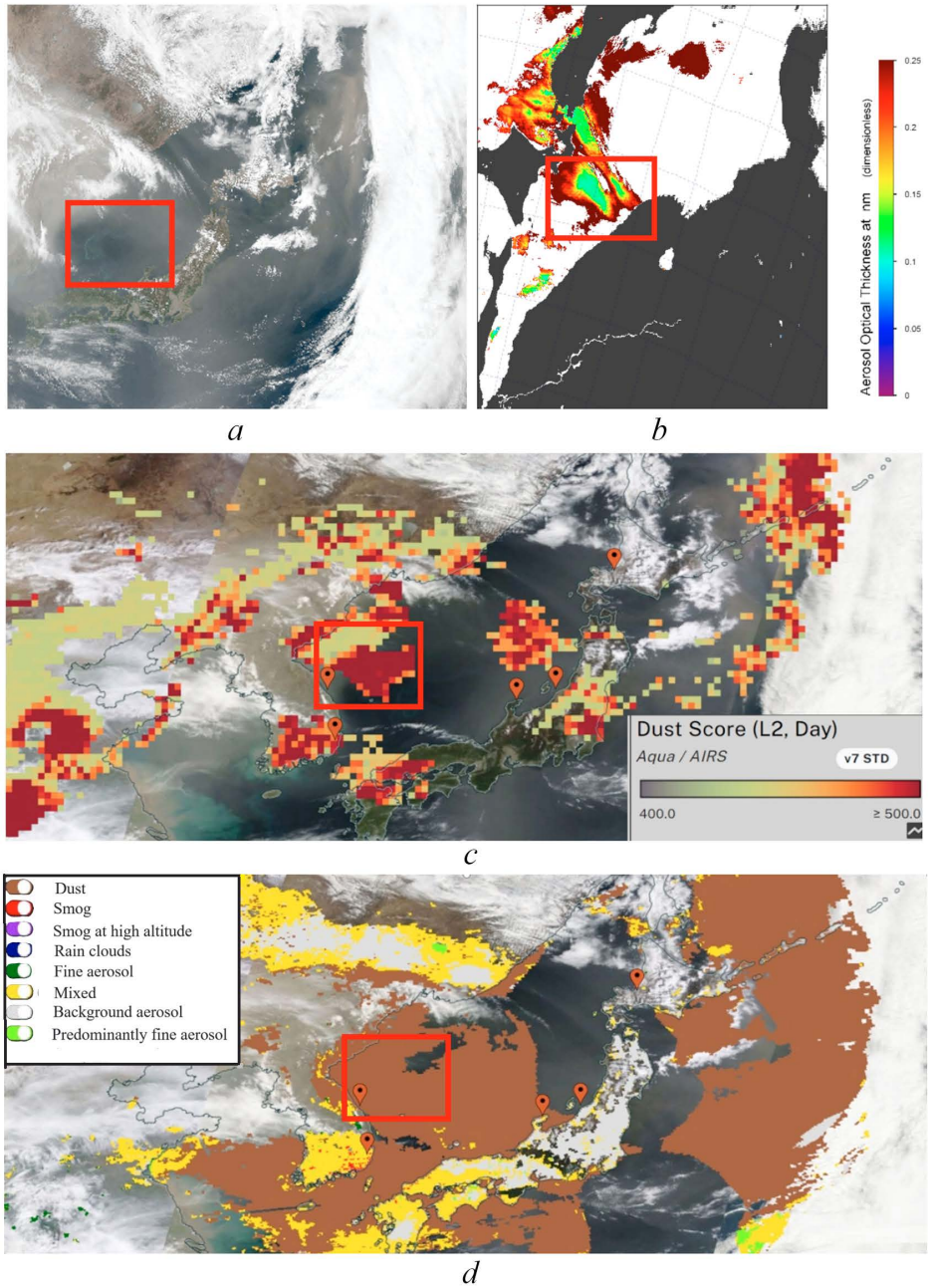

F i g. 2. Satellite image for April 13, 2023: study area from VIIRS/NOAA data (*a*); AOD distribution based on SeaDAS data (*b*); dust distribution from the MODIS/AIRS algorithm (*c*); aerosol-type classification from VIIRS Deep Blue data (*d*) (URL: https://doi.org/10.5067/VIIRS/AERDB_L2_VIIRS_NOAA20.002)

For the highlighted area, the following optical characteristics at a wavelength of 870 nm were obtained from satellite data: AOD = 0.110 ± 0.009, α = 1.046 ± 0.075 for a moderately "clean" atmosphere with background aerosol dominance; AOD = = 0.34 ± 0.034, α = 0.587 ± 0.04 for an atmosphere polluted with dust aerosol. According to AERONET station data from April 13, the average AOD(870 nm) value varied from 0.22 ± 0.02 (Hokkaido_University station) to 0.44 ± 0.03 (Gangneung_WNU and KORUS_UNIST_Ulsan stations). *In situ* data from AERONET stations closest to the dust outflow showed variability of α values from 0.118 to 0.555. The ranges of AOD and α values indicate the dominance of large dust aerosol particles in the atmosphere over the region under study [17, 22, 25].

Table 1 presents the average values of remote sensing reflectance and its standard deviation (SD) for the study region according to VIIRS/NOAA data. From the presented data, it is seen that the standard deviations of $Rrs(\lambda)$ values for the "clean" area with background aerosol are minimal across the entire spectral range, while for dust in the shortwave spectral region they are three times higher. Nevertheless, SD does not exceed 25% of $Rrs(\lambda)$ even for dust, which allows further consideration of average remote sensing reflectance values when analyzing atmospheric correction errors. For dust, calculation results are presented for two periods, April 12–13 and April 21–22.

Table 1

Remote sensing reflectance for the Sea of Japan at different wavelengths (ηm) allowing for standard deviation, based on the VIIRS/NOAA data for April 13, 2023

Type of aerosol	$Rrs(\lambda) \pm$ SD				
	411	445	489	556	667
Background	0.0016 ± 0.0002	0.00235 ± 0.0002	0.0028 ± 0.0002	0.0022 ± 0.0001	0.00054 ± 0.0001
Dust	–0.0023 ± 0.0006	0.00022 ± 0.0004	0.0017 ± 0.0003	0.0015 ± 0.0001	0.00043 ± 0.0001

Upon calculating and approximating the obtained values by a power-law function for the entire Sea of Japan region, an atmospheric correction error of the form λ^{-7} was obtained (Fig. 3). The atmospheric correction error ($\Delta Rrs(\lambda)$) equals the difference between $Rrs(\lambda)$ values for a moderately "clean" atmosphere and $Rrs(\lambda)$ in the presence of dust aerosol. An additional stage of the study for a more accurate assessment of the absorbing properties of dust aerosol was the calculation of the power-law trend of $Rrs(\lambda)$ for April 13 for the AERONET Gangneung_WNU station.

From Fig. 3, it can be seen that the trend of the aerosol absorption power function for the Gangneung_WNU station is close to λ^{-2}. Consequently, the atmospheric correction error (in addition to λ^{-4}) is affected by aerosol light absorption, causing the error of standard atmospheric correction to increase sharply in the ultraviolet spectral region. Thus, the standard algorithm for processing satellite data under dust-transport conditions requires additional

atmospheric correction, where a value proportional to the product of aerosol absorption optical thickness and λ^{-4} should be used as an interpolation function. The proportionality coefficient was determined from the conditions for defining remote sensing reflectance values in the shortwave spectral region. An additional error of the form λ^{-1} can be explained by unfavorable meteorological conditions for satellite scanning.

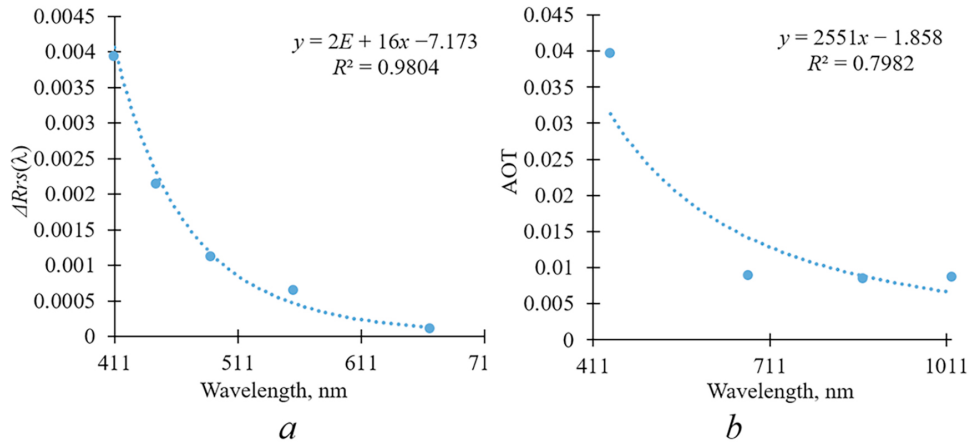

F i g. 3. Variation of the aerosol absorption power function on April 13, 2023 based on the VIIRS/NOAA satellite data (*a*) and the international AERONET network data (*b*) for the Gangneung_WNU station

Two dust transport events from the Gobi Desert were recorded over the Sea of Japan on April 8–13 and 17–22. Maximum concentrations of dust aerosol according to satellite data were observed during April 12–13 and 21–22. The next stage of the research is the analysis of dust aerosol transport using data from the 2378-channel infrared sounding system AIRS. Maps of atmospheric loading with dust aerosol particles confirm that the source regions of dust aerosol origin are the Gobi and Taklamakan deserts (Fig. 4). Analysis of aerosol loading showed that the dust storm began on April 8 in the Gobi Desert. The peak concentration of dust aerosol particles (Dust Score) according to MODIS/AIRS data was observed in the Sea of Japan on April 11 over the eastern AERONET stations Noto, Niigata, and Hokkaido_University (highlighted with markers), and over the entire water area on April 12 (Fig. 4).

To assess the scale of dust impact on the surface layer of the Sea of Japan, publicly available satellite pseudo-color images on the EOSDIS platform, as well as remote sensing reflectance, were analyzed (Fig. 5). The dust concentration over the water area is so high that satellite data processing algorithms for all days considered cannot retrieve sea reflectance for the entire water area even in the absence of clouds, recognizing dust areas as dense cloud layers. This effect is particularly evident in the satellite image from April 12, when with an almost completely cloud-free Sea of Japan, remote sensing reflectance values determined by satellite algorithms are absent for the entire water area (Fig. 5, *c*, *d*).

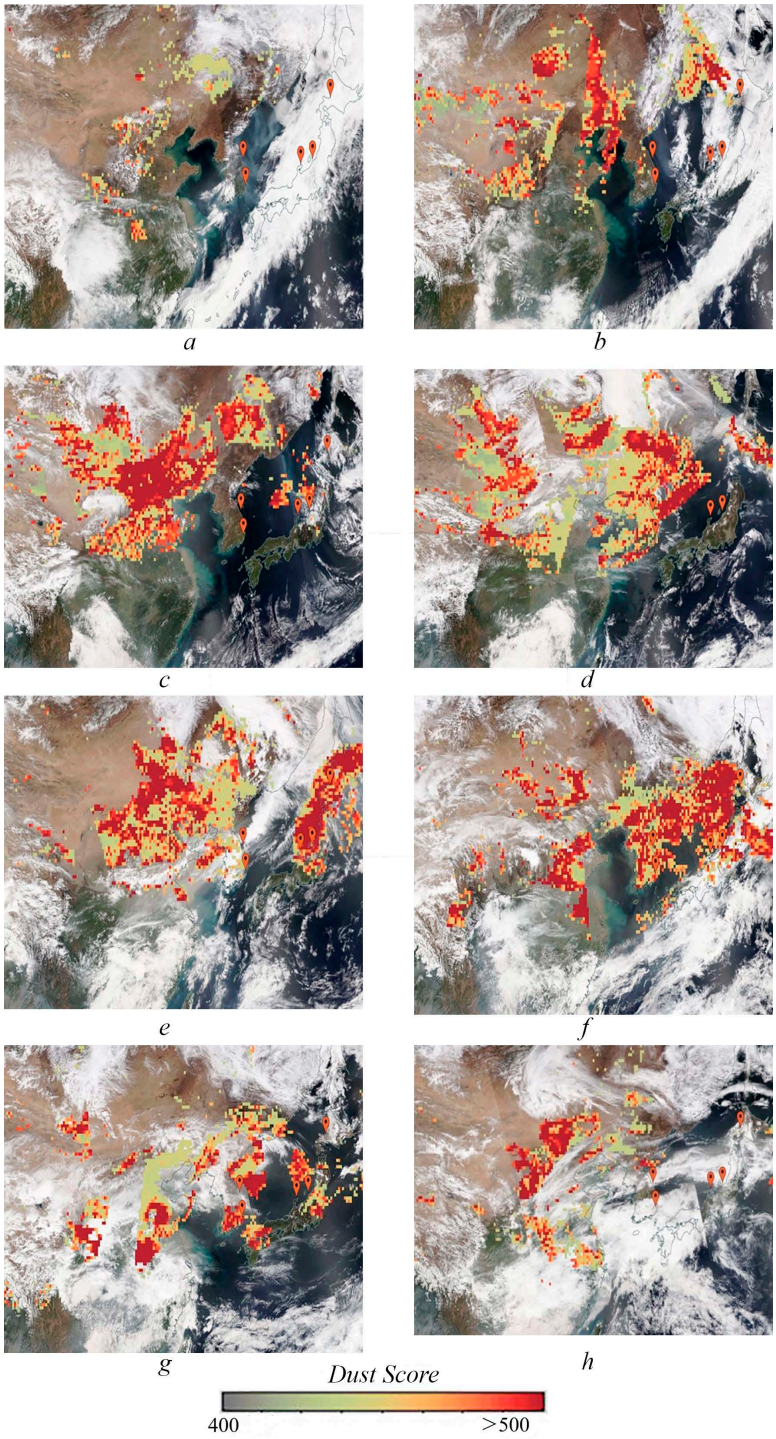

F i g. 4. Dust aerosol loading based on MODIS Aqua/AIRS data on: *a* – April 7, *b* – April 8, *c* – April 9, *d* – April 10, *e* – April 11, *f* – April 12, *g* – April 13, and *h* – April 14, 2023 (https://aqua.nasa.gov/modisonet.gsfc.nasa.gov/)

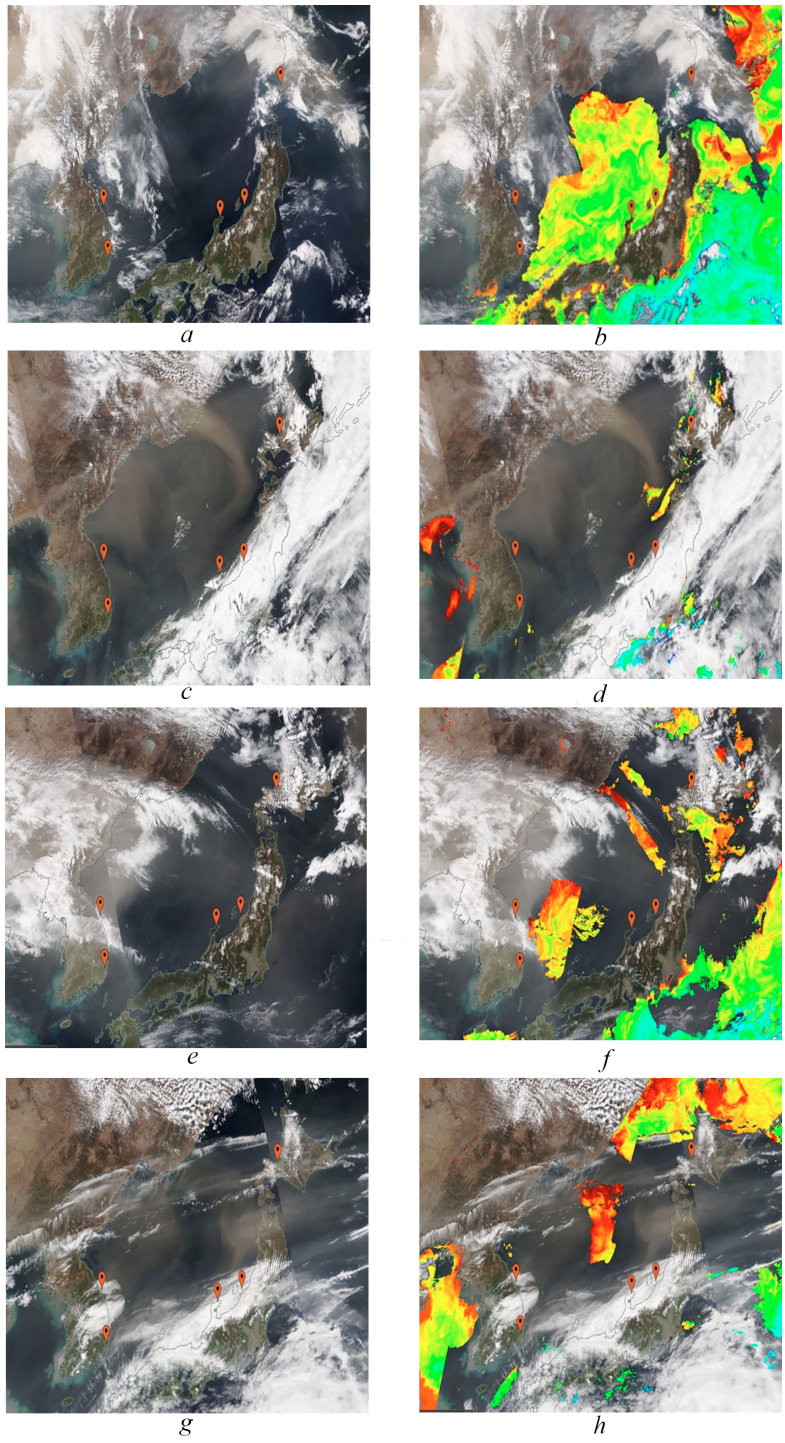

F i g. 5. Survey area in the Sea of Japan derived from VIIRS/NOAA satellite imagery. Sea areas in pseudo-colors (left column) and remote sensing reflectance (right column) on various dates: *a*, *b* – April 10; *c*, *d* – April 12; *e*, *f* – April 13; *g*, *h* – April 21 (https://doi.org/10.5067/VIIRS/AERDB_L2_VIIRS_NOAA20_NRT.002)

To determine the altitude of dust aerosol transport, an analysis of backward air mass trajectory data using the HYSPLIT model for the study period was carried out (Fig. 6). Note that dust transport occurred at all altitudes from 500 to 3000 m (red color indicates 500 m, blue – 1500 m, green – 3000 m). It is evident that on almost all dates considered, aerosol transport over the Sea of Japan water area originated from the Gobi and Taklamakan deserts.

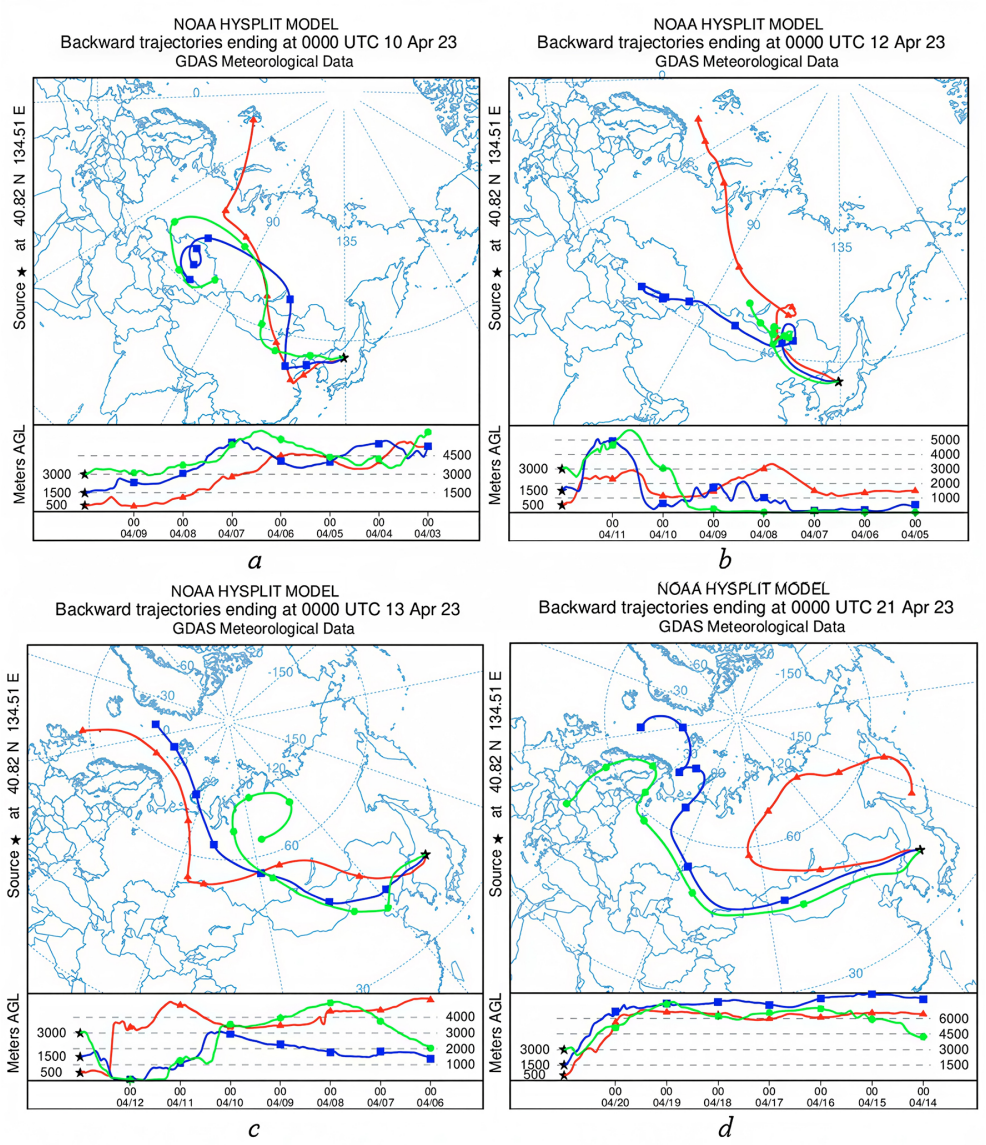

F i g. 6. Back trajectories of airflow transport based on the HYSPLIT modeling results: *a* – April 10, *b* – April 12, *c* – April 13 and *d* – April 21, 2023 (https://www.ready.noaa.gov/HYSPLIT.php)

Data on the concentration of suspended particles (PM10 and PM2.5) from the SILAM model showed elevated (relative to the monthly average) values for the Sea of Japan region (Fig. 7). According to the analysis of the AQI characteristics,

high values (AQI = 175) were recorded on April 10 over the Hokkaido_University station and on April 11 over the Gangneung_WNU station. However, these were local maxima, and over most of the water area and coast, AQI = 100 ± 10 corresponded to a satisfactory level of air pollution.

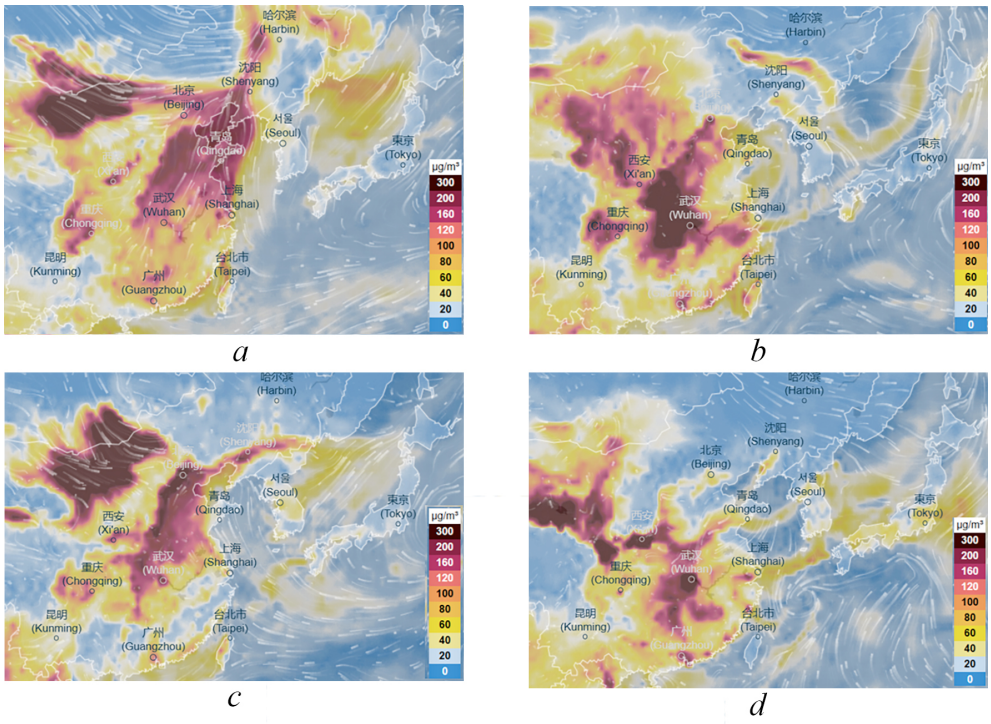

Fig. 7. Concentration of PM10 particles in the atmosphere based on SILAM model data: *a* – April 10, *b* – April 12, *c* – April 13 and *d* – April 21, 2023 (https://thredds.silam.fmi.fi/thredds/catalog/catalog.html)

Based on an array of *in situ* optical characteristics obtained at AERONET stations, it was shown that the maximum AOD values in April at all wavelengths coincided with the dates of dust aerosol transport, April 13 and 21. Dust aerosol has the greatest effect on the longwave part of the spectrum. In the graphs of Fig. 8, from the peaks of AOD values at wavelengths of 870 and 1020 nm, it is seen that the entire period from April 10 to 26 is characterized by a turbid atmosphere. On the dust transport days of April 12–13 and 21–22, AOD(870) and AOD(1020) reached values of 0.5–0.6, which is more than 5 times higher than AOD values observed in the same month on days with a clean atmosphere.

Also, according to measurements from the AERONET network, based on data on the Angstrom exponent, conclusions can be drawn about particle size distribution from the ratio of different wavelengths (Table 2). As can be seen, the smallest difference in values between background and dust aerosol in the atmosphere is observed for α(440–675) at the Noto station. The greatest difference in values (4 times) is observed for α(500–870) at the Gangneung_WNU station. All spectral values of the Angstrom exponent confirm the dominance of large aerosol particles during the April dust transport over the Sea of Japan.

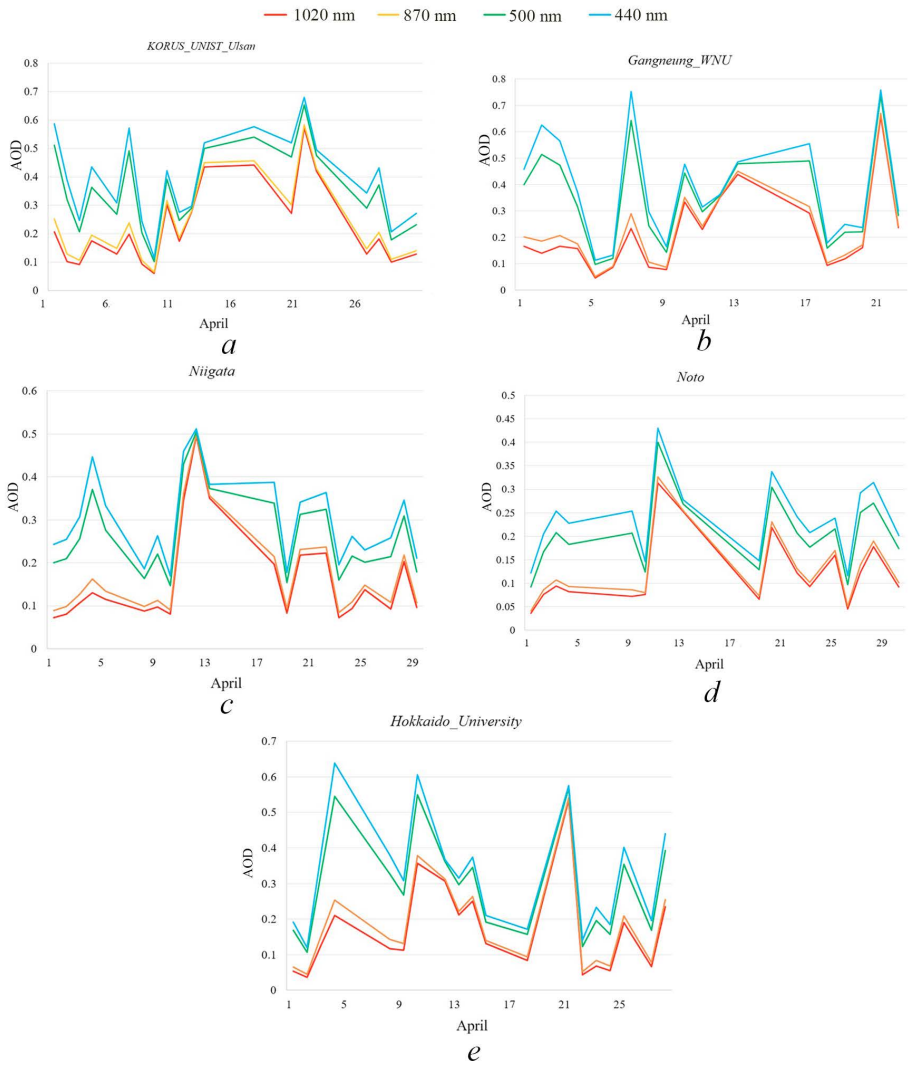

F i g. 8. Spectral variability of AOD values for April 2023 based on AERONET station data: KORUS_UNIST_Ulsan (*a*); Gangneung_WNU (*b*); Noto (*c*); Niigata (*d*); Hokkaido_University (*e*)

V3 inversion products presented on the AERONET network platform contain data on the variability of single-scattering albedo (Λ). According to the analysis of albedo values, dust aerosol possesses predominantly absorbing or scattering properties. The combination of high (1.5–2 times higher than background) AOD values and low (less than 0.7) values of α and Λ (especially in the shortwave region) is an indicator of the presence of absorbing dust aerosol in the atmosphere. On days with the highest dust concentration over the studied stations, Λ value at 440 nm decreased to 0.85.

Table 2

Spectral values of the Angstrom parameter (α) at the AERONET network stations for the Sea of Japan in the presence of background and dust aerosol in the atmosphere

AERONET stations	Type of aerosol					
	Background	Dust	Background	Dust	Background	Dust
	α(440–675)		α(500–870)		α(340–440)	
Hokkaido_University	1.12	0.62	1.07	0.58	0.92	0.55
Noto	1.04	0.70	0.92	0.60	0.90	0.53
Niigata	1.25	0.58	1.12	0.48	1.11	0.60
Gangneung_WNU	1.18	0.33	1.12	0.28	0.94	0.31
KORUS_UNIST_Ulsan	1.17	0.41	1.07	0.34	1.04	0.46

Conclusion

A comparative analysis of optical-characteristic values at AERONET stations located on the coast of the Sea of Japan allowed the identification of dates in April 2023 when dust aerosol had the maximum impact on remotely determined water parameters of the study region. *In situ*, satellite, and model data confirmed different aerosol loading over the "clean" (presence of background aerosol) and completely dust-covered areas of the Sea of Japan water area, as well as spatial variability of the main aerosol optical characteristics during the observation of dust transport from the Gobi and Taklamakan deserts. According to satellite data, at a wavelength of 870 nm for the area with background aerosol AOD = 0.110 ± 0.009, α = 1.046 ± 0.075; for the heavily dust-polluted area AOD = 0.34 ± 0.034, α = 0.587 ± 0.04. *In situ* data from AERONET stations closest to the dust outflow showed variability of the Angstrom exponent within the range of 0.118–0.555.

It was indicated that on days with anomalously intensive transport from Asia, the dust concentration over the water area is so high that it is impossible to retrieve remote sensing reflectance for the entire water area using satellite data processing algorithms even in the absence of clouds, as dust areas are recognized as dense cloud layers.

As a result of a comparative analysis of satellite and photometric *in situ* data, it was confirmed that the error of standard atmospheric correction increases sharply in the ultraviolet spectral region during dust transport. Approximation of the obtained values by a power-law function showed an atmospheric correction error of the form λ^{-7} for the entire Sea of Japan region. An analytical assessment of the error in satellite measurements of sea remote sensing reflectance according to VIIRS/NOAA data for the studied period constituted approximately 70% in the shortwave spectral region, up to 47% in the visible spectral region, and 24% in the longwave region compared to *in situ* data.

In subsequent studies, it is planned to analyze a larger number of dust transport events from Asia and their impact on the hydro-optical characteristics of the Sea of Japan using not only *in situ* measurements of atmospheric parameters but also satellite remote sensing reflectance data.

REFERENCES

1. Song, H., Zhang, K., Piao, S. and Wan, S., 2016. Spatial and Temporal Variations of Spring Dust Emissions in Northern China over the Last 30 Years. *Atmospheric Environment,* 126, pp. 117-127. https://doi.org/10.1016/j.atmosenv.2015.11.052

2. Wang, H., Zhao, T., Zhang, X. and Gong, S., 2011. Dust Direct Radiative Effects on the Earth-Atmosphere System over East Asia: Early Spring Cooling and Late Spring Warming. *Chinese Science Bulletin*, 56(10), pp. 1020-1030. https://doi.org/10.1007/s11434-011-4405-3

3. Yu, H., Yang, Y., Wang, H., Tan, Q., Chin, M., Levy, R.C., Remer, L.A., Smith, S.J., Yuan, T. [et al.], 2020. Interannual Variability and Trends of Combustion Aerosol and Dust in Major Continental Outflows Revealed by MODIS Retrievals and CAM5 Simulations during 2003–2017. *Atmospheric Chemistry and Physics*, 20(1), pp. 139-161. https://doi.org/10.5194/acp-20-139-2020

4. Li, Y. and Wang, W., 2024. Long-Range Transport of a Dust Event and Impact on Marine Chlorophyll-*a* Concentration in April 2023. *Remote Sensing*, 16(11), 1883. https://doi.org/10.3390/rs16111883

5. Shanmugam, P. and Ahn, Y.-H., 2007. New Atmospheric Correction Technique to Retrieve the Ocean Colour from SeaWiFS Imagery in Complex Coastal Waters. *Journal of Optics A: Pure and Applied Optics*, 9(5), pp. 511-530. https://doi.org/10.1088/1464-4258/9/5/016

6. Fukushima, H. and Toratani, M., 1997. Asian Dust Aerosol: Optical Effect on Satellite Ocean Color Signal and a Scheme of Its Correction. *Journal of Geophysical Research: Atmospheres*, 102(D14), pp. 17119-17130. https://doi.org/10.1029/96JD03747

7. Zvalinsky, V.I., Lobanova, P.V., Tishchenko, P.Ya., Lobanov, V.B. and Makhovikov, A.D., 2022. Estimation of Primary Production in the Northern Part of the Sea of Japan in Various Seasons by Ship- and Satellite-Based Observations. *Oceanology*, 62(5), pp. 630-645. https://doi.org/10.1134/S0001437022050216

8. Shtraichert, E.A., Zakharkov, S.P., Gordeychuk, T.N. and Shambarova, Yu.V., 2014. Chlorophyll-a Concentration and Bio-Optical Characteristics in Peter the Great Bay (Sea of Japan) during Winter-Spring Phytoplankton Bloom. *Sovremennye Problemy Distantsionnogo Zondirovaniya Zemli iz Kosmosa*, 11(1), pp. 148-162 (in Russian).

9. Salyuk, P.A., Stepochkin, I.E., Shmirko, K.A. and Golik, I.A., 2024. Using Satellite Multi-Angle Polarization Measurements to Characterize Atmospheric Aerosol above Bohai Bay. *Advances in Space Research*, 73(1), pp. 514-522. https://doi:10.1016/j.asr.2023.10.007

10. Bukin, O.A., Pavlov, A.N., Salyuk, P.A., Kulchin, Yu.N., Shmirko, K.A., Stolyarchuk, S.Yu. and Bubnovskii, A.Yu., 2007. Peculiarities of the Aerosol Vertical Distribution during the Passage of Dust Storms over the Peter the Great Bay in 2006 and Their Influence on Phytoplankton Communities in the Japan Sea. *Atmospheric and Oceanic Optics*, 20(4), pp. 306-312.

11. Dubovik, O. and King, M.D., 2000. A Flexible Inversion Algorithm for Retrieval of Aerosol Optical Properties from Sun and Sky Radiance Measurements. *Journal of Geophysical Research: Atmospheres*, 105(D16), pp. 20673-20696. https://doi.org/10.1029/2000JD900282

12. Barnes, W.L., Xiong, X. and Salomonson, V.V., 2003. Status of Terra MODIS and Aqua Modis. *Advances in Space Research*, 32(11), pp. 2099-2106. https://doi.org/10.1016/S0273-1177(03)90529-1

13. Cao, C., Xiong, J., Blonski, S., Liu, Q., Uprety, S., Shao, X., Bai, Y. and Weng, F., 2013. Suomi NPP VIIRS Sensor Data Record Verification, Validation, and Long-Term Performance Monitoring. *Journal of Geophysical Research: Atmospheres*, 118(20), pp. 664-678. https://doi:10.1002/2013JD020418

14. Wang, W., Mao, F., Pan, Z., Du, L. and Gong, W., 2017. Validation of VIIRS AOD through a Comparison with a Sun Photometer and MODIS AODs over Wuhan. *Remote Sensing*, 9(5), 403. https://doi.org/10.3390/rs9050403

15. Choi, T., Cao, C., Blonski, S., Shao, X. and Wang, W., 2024. NOAA-20 VIIRS On-Orbit Reflective Solar Band Radiometric Calibration Five-Year Update. *IEEE Transactions on Geoscience and Remote Sensing*, 62, pp. 1-10. https://doi.org/10.1109/TGRS.2024.3363661

16. Lee, J., Hsu, N.C., Kim, W.V., Sayer, A.M. and Tsay, S.-C., 2024. VIIRS Version 2 Deep Blue Aerosol Products. *Journal of Geophysical Research: Atmospheres*, 129(6), e2023JD040082. https://doi.org/10.1029/2023JD040082

17. Papkova, A.S., Shybanov, E.B. and Kalinskaya, D.V., 2024. The Effect of Dust Aerosol on Satellite Data from Different Color Scanners. *Physical Oceanography*, 31(5), pp. 720-735.

18. Dubovik, O., Holben, B.N., Eck, T.F., Smirnov, A., Kaufman, Y.J., King, M.D., Tanré, D. and Slutsker, I., 2002. Variability of Absorption and Optical Properties of Key Aerosol Types Observed in Worldwide Locations. *Journal of the Atmospheric Sciences*, 59(3), pp. 590-608. https://doi.org/10.1175/1520-0469(2002)059<0590:VOAAOP>2.0.CO;2

19. Tiwari, A., Soni, V.K., Jena, C., Kumar, A., Bist, S. and Kouznetsov, R., 2022. Pre-Operational Validation of Air Quality Forecasting Model SILAM for India. *Journal of Pollution Effects &Control*, 10(4), 343. https://doi.org/10.35248/2375-4397.22.10.343

20. Dementeva, A.L., Zhamsueva, G.S., Zayakhanov, A.S., Tcydypov, V.V., Starikov, A.V. and Balzhanov, T.S. 2023. Variability of Aerosol Concentrations of Fractions PM10 and PM2.5 in the Atmosphere Surface Layer at the Reference Monitoring Station Boyarsky. In: SPIE, 2023. *Proceedings of SPIE 12780, 29th International Symposium on Atmospheric and Ocean Optics: Atmospheric Physics*, 127805X. https://doi.org/10.1117/12.2690736

21. Griffin, D.W. and Kellogg, C.A. 2004. Dust Storms and Their Impact on Ocean and Human Health: Dust in Earth's Atmosphere. *EcoHealth*, 1(3), pp. 284-295. https://doi.org/10.1007/s10393-004-0120-8

22. Middleton, N. and Kang, U., 2017. Sand and Dust Storms: Impact Mitigation. *Sustainability*, 9(6), 1053. https://doi.org/10.3390/su9061053

23. Sofiev, M., Siljamo, P., Valkama, I., Ilvonen, M. and Kukkonen, J., 2006. A Dispersion Modelling System SILAM and Its Evaluation against ETEX Data. *Atmospheric Environment*, 40(4), pp. 674-685. https://doi.org/10.1016/j.atmosenv.2005.09.069

24. Frohn, L.M., Geels, C., Andersen, C., Andersson, C., Bennet, C., Christensen, J.H., Im, U., Karvosenoja, N., Kindler, P.A. [et al.], 2022. Evaluation of Multidecadal High-Resolution Atmospheric Chemistry-Transport Modelling for Exposure Assessments in the Continental Nordic Countries. *Atmospheric Environment*, 290, 119334. https://doi.org/10.1016/j.atmosenv.2022.119334

25. Kalinskaya, D.V. and Papkova, A.S., 2023. Variability of the Water-Leaving Radiance under the Conditions of Dust Transport by the Satellite Sentinel-3 Data on the Example of the Black Sea and Sevastopol. *Physical Oceanography*, 30(3), pp. 369-383. https://doi.org/10.29039/1573-160X-2023-3-369-383

Submitted 18.07.2025; approved after review 16.09.2025;
accepted for publication 10.11.2025.

About the authors:

Daria V. Kalinskaya, Junior Researcher, Marine Hydrophysical Institute of RAS (2 Kapitanskaya Str., Sevastopol, 299011, Russian Federation), **Scopus Author ID: 56380591500**, **SPIN-code: 2622-1010**, **WoS ResearcherID: G-2959-2017**, kalinskaya@mhi-ras.ru

Anna S. Papkova, Junior Researcher, Marine Hydrophysical Institute of RAS (2 Kapitanskaya Str., Sevastopol, 299011, Russian Federation), CSc. (Phys.-Math.), **Scopus Author ID: 57203015832**, **SPIN-code: 1683-7685**, **WoS ResearcherID: AAP-3248-2020**, hanna.papkova@gmail.com

Contribution of the co-authors:

Daria V. Kalinskaya – conceptualization and curation, methodology, data collection, investigation, visualization, preparatory drafting

Anna S. Papkova – methodology, investigation, data collection, formal analysis, visualization, preparatory drafting, review and editing

The authors have read and approved the final manuscript.
The authors declare that they have no conflict of interest.